Research Article

iMedPub Journals
http://www.imedpub.com/

Dual Diagnosis: Open Access
ISSN 2472-5048

2019
Vol.4 No.1: 1

Dynamic Weighted Functional Connectivity Analysis for Autism Spectrum Disorders Classification

Hongliang Zou[1*] and Jian Yang[2]

[1]PCA Lab, Key Lab of Intelligent Perception and Systems for High-Dimensional Information of Ministry of Education, China
[2]Jiangsu Key Lab of Image and Video Understanding for Social Security, School of Computer Science and Engineering, Nanjing University of Science and Technology, Nanjing 210094, China

[*]**Corresponding author:** Hongliang Zou, PCA Lab, Key Lab of Intelligent Perception and Systems for High-Dimensional Information of Ministry of Education, China, E-mail: hongliangzou@126.com

Received date: June 9, 2019; **Accepted date:** June 24, 2019; **Published date:** July 03, 2019

Citation: Hongliang Z, Yang J (2019) Dynamic Weighted Functional Connectivity Analysis for Autism Spectrum Disorders Classification. Dual Diagn. Open Acc Vol.4 No.1: 1.

Abstract

Autism spectrum disorder (ASD) is a serious neurodevelopmental disorder for children and adolescent. Accurate diagnosis of ASD plays a key role in improving the life quality of individuals with ASD and reducing the burden of healthcare system. Currently, Functional Connectivity (FC) analysis based on functional Magnetic Resonance Imaging (fMRI) has become a popular approach in diagnosis of ASD, but majority of previous studies were based on the assumption that FC is stationary throughout the entire scan session, ignoring the fluctuations over the course of the scan. Previously sliding window based Dynamic FC (DFC) method was proposed to estimate the dynamic changes, but it has a limitation that all observations within the window are weighted equally. To address the issue, we have proposed Dynamic Weighted FC (DWFC) method in this study to extract features from resting-state fMRI (rs-fMRI) and applied it to distinguishing ASD patients from Normal Controls (NC). Experiments were carried on subjects from the Autism Brain Imaging Data Exchange (ABIDE) database. The classification accuracy is 0.8525 and 0.8061 on two independent datasets. Results showed that the proposed method significantly outperformed conventional FC and DFC approaches, as well as other state-of-the-art ASD classification methods, which suggests this method as a promising computer-acid diagnosis tool for ASD.

Keywords: ASD; Dynamic Weighted FC; Rs-fMRI; Two independent datasets; Computer-acid Diagnosis

Introduction

Autism Spectrum Disorder (ASD) is a prevalent neurodevelopmental disorder characterized by significant impairments of social-communication deficits and stereotyped or repetitive behaviors and interests [1,2]. At present, the clinical diagnosis of ASD is mainly behavior-based and depended on some clinical measures that quantify the severity of the disorder [3,4]. However, the approach may be not accurate because many behavioral phenotypes are associated with numerous other psychological and psychiatric disorders due to the similar symptom [1,5,6]. To address this issue, combined brain imaging and machine learning methods have been proposed as aided diagnostic tools [7,8] to automatically identify ASD in a non-invasive fashion.

Machine learning techniques have been widely used in the diagnosis of various diseases, such as mild cognitive impairment [9], Alzheimer ' s disease [10], Parkinson disease [11], schizophrenia [12,13] and ASD [3,4]. Functional magnetic resonance imaging (fMRI), which measures synchronized brain activity via blood oxygenation, holds great promises for exploring the *in vivo* neuronal underpinnings of ASD. Functional connectivity (FC) describes temporal correlation among spatially distant brain regions and resting-state fMRI (rs-fMRI) is commonly used to investigate brain disorders by using pattern classifiers. For example, Iidaka [14] classified autism and control based on resting-state FC with neural network; Chen et al. [15] using FC network based on two different frequency bands to identify individuals with ASD; Zhao et al. [3] proposed a machine learning-based method with feature fusion via hierarchical supervised local Canonical Correlation Analysis (CCA) for diagnosis of ASD based on structure Magnetic Resonance Imaging (sMRI) and rs-fMRI; recently, Subbaraju and colleagues [16] proposed a new spatial feature based detection method, which extracts discriminative features based on connectivity for ASD classification based on rs-fMRI data.

Although some promising results were obtained using these methods, all of these studies were based on the assumption that FC is stationary throughout the entire scan session, which may be not true, because some studies have shown that FC among brain regions is time-varying in fact.

Hence a better method is to involve the dynamic characteristics of FC. The most common approach for estimating these dynamic changes is to use the sliding window technique. But this approach still has the drawback, i.e., all observation within the window is weighted equally [17-19], which overlooks the difference of different time points contributing to the

connection. To address the issue, a Dynamic Weighted FC (DWFC) method is proposed in current study to distinguish ASD patients from normal controls based on resting-state fMRI. Briefly, DWFC was established using sliding window (different time points within each window with different weight) technology in the first. The advantages of this measure includes: (1) time-varying character is captured in the process of establishing connectivity network; (2) the different contributions at different time points are quantified through different weights. Then, variance matrix was calculated to extract features. Subsequently, to remove the redundancy information and select the most relevant features with the target from feature set, the feature selection strategy was adopted. Support vector machine (SVM) has been applied in classifying individuals with ASD from normal controls.

Materials and Methods

Figure 1 shows a flowchart of the proposed classification framework, which mainly including the following procedures: Image obtain and processing, construction of DWFC, feature extraction and selection, and classification.

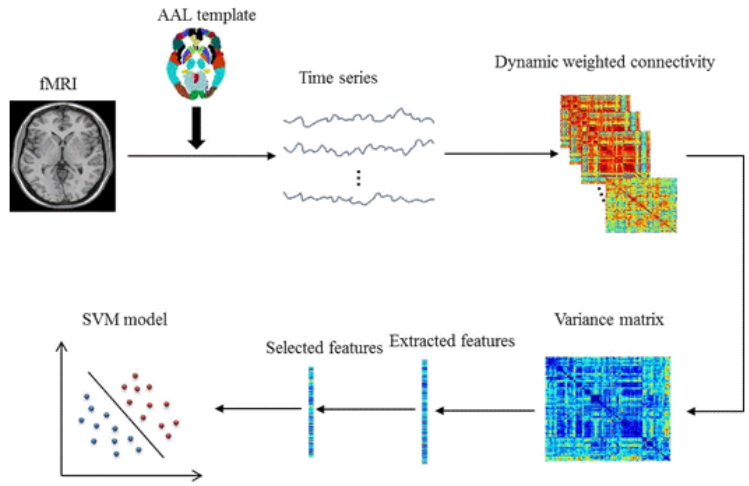

Figure 1: Flowchart of the proposed method.

Subjects

The data used in this work was selected from the publicly available Autism Brain Imaging Data Exchange (ABIDE) database [20], which was established as a data repository for facilitating scientific discovery and accelerate our understanding of the neural bases of autism. Subjects with were drawn from the following two centers have the largest sample size in ABIDE database, including New York University (NYU) Langone Medical Center and University of California, Los Angeles (UCLA). Specifically, we focused on rs-fMRI data. The demographic information and scanning parameters of the data were summarized in **Table 1**. For more detailed information about the data collection, please refer to http://fcon_1000.projects.nitrc.org/indi/abide/.

Table 1: The demographic information and acquisition parameters of images used in current study.

Center		NYU		UCLA
Variable	ASD	NC	ASD	NC
Number of subjects	58	64	55	43
Gender (male/female)	51/7	46/18	49/6	37/6
Age	10.48 ± 2.40	11.19 ± 2.54	12.02 ± 1.93	12.14 ± 1.52
MRI vendor		Siemens		Siemens
TR (ms)		2000		3000
TE (ms)		15		28
Flip angle (deg)		90		90
Voxel size (mm^3)	3.0 × 3.0 × 4.0		3.0 × 3.0 × 4.0	
Volumes		180		120

Pre-processing

Standard fMRI image preprocessing was carried out using the Data Processing Assistant for Resting-State fMRI (DPARSF) [21] toolbox, which is based on Statistical Parametric Mapping (SPM8) (http://www.fil.ion.ucl.ac.uk/spm) and Resting-State fMRI Data Analysis Toolkit [22] (REST, http://www.restfmri.net). For each subject, the first 10 images of the functional images were discarded before any further analysis to ensure magnetization equilibrium. Slice timing correlation, realignment and normalization were then performed. Next, the images were normalized into the Montreal Neurological Institute (MNI) space. The resulting images were temporally filtered with a band-pass filter (0.01-0.08 Hz) [23]. The rs-fMRI image was regressed to reduce the effects of nuisance signals including six head-motion parameters, white matter signals and cerebrospinal fluid signals. Then, the automated anatomical

labeling (AAL) [24] template was used to divide the rs-fMRI image into 116 regions of interesting (ROIs), including 90 cerebrum regions (45 in each hemisphere) and 26 cerebellum regions (9 in each cerebellar hemisphere and 8 in the vermis). The mean time series of each brain region were obtained for each individual by averaging the fMRI time series within the region [25].

Suppose $X_i = (x_i(1), x_i(2), ..., x_i(L))$and $X_j = (x_j(1), x_j(2), ..., x_j(L))$ are two L length time series of brain region i and j, the Pearson's correlation (PC) between them can calculated as$PC_{ij} = \frac{\mathrm{cov}(X_i, X_j)}{\sigma x_i \sigma x_j}$ (1)Where, cov covers σx_i and σx_j are the standard deviation of ith and jth time series, respectively.

Although above measure can capture the interaction between regions, it depends on the assumption that the connectivity remains constant throughout the entire scan session, which ignores the fact that an individual subject is likely to engage in slightly different mental activities at different time points. Some studies have reported that the connectivity could change over the course of the scan, and these dynamics can also be linked to changes in human behavior [26,27].

To estimate the dynamic change of time series, sliding window strategy is adopted in this work. Dynamic FC between two time series was computed with pairwise Pearson's correlation using rectangular sliding windows of length N TRs and step size 1 TR, thus generating T=L-N+1 windows. The k th window pairwise correlation of two regions can be computed as:

$$DFC_{ij}^{(k)} = \frac{\mathrm{cov}(X_i^{(k)}, X_j^{(k)})}{\sigma X_{i(k)} \sigma X_{j(k)}}, (k = 1, 2, ..., T) \quad (2)$$ Where $X_i^{(k)}$ represent the k -th window in i -th time series, and analogously for $X_j^{(k)}$ However, the approach has shortcoming, since all observations within the time window is weighted equally. To better capture the characteristics of different time instances that could generate different contributions to connectivity, dynamic weighted FC (DWFC) method was proposed in this work. In this approach, the interaction between i-th and j-th brain region within k-th window in DWFC model can be formulated as shown in **Figure 2:**

$$DFC_{ij}^{(k)} = \frac{\Sigma[w(\tau)xi^{(k)}(\tau) - \mu i^{(k)}] . [w(\tau)xj^{(k)}(\tau) - \mu j^{(k)}]^N_{\tau=1}}{\sqrt{\sum_{\tau=1}^{N}[w(\tau)x_i^{(k)}(\tau) - \overline{\mu_i^{(k)}}}\sqrt{\sum_{\tau=1}^{N}[w(\tau)x_i^{(k)}(\tau) - \overline{\mu_i^{(k)}}}}$$

(3)Where $\overline{\mu_i^{(k)}} = \sum_{\tau=1}^{N}[w(\tau)x_i^{(k)}(\tau)$and $x_i^{(k)}(\tau)$ represent the τth element within k-th window in i-th time series. Among various financial studies, most operators would judge the information from recent events as more valuable than from remote ones for both descriptive and forecasting purpose [28], so weighted recent events more heavily. In this work, to take advantage of the time information within the window, we defined$w(\tau) = \frac{\tau}{L}$.

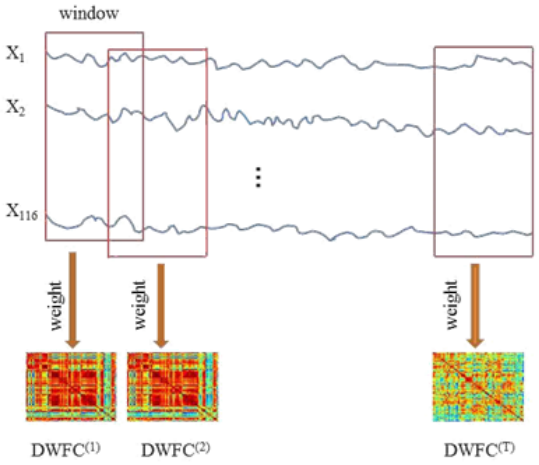

Figure 2: The calculation process of DWFC.

Feature eXtraction and feature selection

The variance of the time series of correlation coefficient obtained by Eqn. 3 was computed to assess temporal variability according to the following equation:

$$V_{ij} = \frac{1}{T-1}\sum_{k=1}^{T}(DWFC_{ij}^{(k)} - \frac{1}{T}\sum_{k=1}^{T}DWFC_{ij}^{(k)})^2 \quad (4)$$

Figure 3 illuminates how to obtain the variance of the correlation between two different regions. Due to symmetry, only the upper triangular of the variance matrix obtained by Eqn.4 was used. For each sample, all elements in upper triangular part of the variance matrix were concatenated to form a feature vector with 116 × (116-1)/2=6670 elements. Feature extraction and feature selection are the two important aspects in machine learning and image processing areas. In order to avoid the curse of dimensionality, the feature selection strategy was adopted to remove the irrelevant and redundancy

information, which will lead to poor classification performance. In current study, the LASSO (Least Absolute Shrinkage and Selection Operator) [29] was utilized to select a small feature subset relevant to ASD disease.

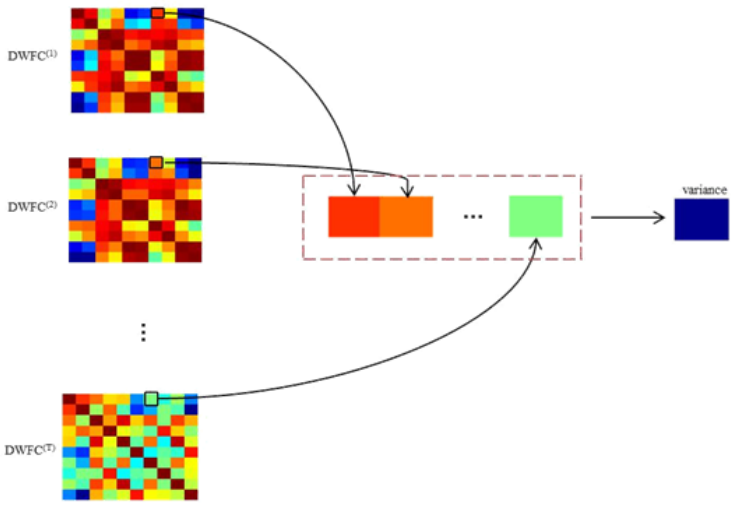

Figure 3: Illuminates the calculation process of variance.

Classification

Support vector machine (SVM) [30-32] is an effective tool in machine learning and pattern recognition fields. It has been widely used in bioinformatics [33,34] and diagnosis of diseases [13,35,36]. The basic idea of SVM is to establish a hyper-plane to maximize the margin between the positive sample and negative sample. We use SVM with a simple linear kernel in current study.

Given the limited number of samples in the dataset, the Leave-One-Out cross-validation (LOOCV) approach was used to evaluate the performance of the proposed framework. Specifically, suppose that there are m subjects in the dataset, then m-1 subjects are used for training; the remaining one is used for testing. The entire process was repeated m times, each time leaving out a different subject for testing.

Performance metric

The proposed method was evaluated based on data scanned at two different centers (NYU Langone Medical Center and University of California, Los Angeles) in this section. We employed the following six different metrics to evaluate its diagnostic power for ASD: Classification Accuracy (ACC), Sensitivity (SEN), Specificity (SPE), Positive Predictive Value (PPV), Negative Predictive Value (NPV), F-score (F). They are defined respectively as,

$$\begin{cases} ACC = \dfrac{TP+TN}{TP+FP+TN+FN} \\ SEN = \dfrac{TP}{TP+FN} \\ SPE = \dfrac{TN}{TN+FP} \\ PPV = \dfrac{TP}{TP+FP} \\ NPV = \dfrac{TN}{TN+FN} \\ F = 2 \times \dfrac{precision \times recall}{precision + recall} \end{cases} \quad (5)$$

Where TP, FP, TN, FN denote the number of true positive, false positive, true negative and false negative, respectively.

Precision=PPV=$\frac{TP}{TP+FP}$; recall=SEN=$\frac{TP}{TP+FN}$ (6)

Besides, to better evaluate the classification performance of the proposed model on imbalanced classes of these datasets, the area under receiver operating characteristic (AUC) was also adopted.

Results

Classification performance

The proposed DWFC was compared with Pearson's correlation (PC) and DFC measure. The results by these methods were summarized in **Tables 2 and 3**. It can be observed that our DWFC can achieve the best classification performance compared to other methods. Specifically, the yield classification accuracy of the proposed method is 0.8525 and 0.8061 on NYU and UCLA,

respectively, whereas the best classification accuracy is 0.6885, 0.7143 and 0.7951, 0.7857 for PC and DFC. To confirm whether our method has statistical significance, permutation test (1000 times) was performed, the corresponding p-values are 0.001 (NYU) and 0.004 (UCLA), respectively, which verified the efficacy of proposed model.

Table 2: The achieved classification results using different methods on NYU dataset.

Method	AAC	SEN	SPE	PPV	NPV	F	AUC
PC	0.6885	0.6552	0.7188	0.6786	0.697	0.6667	0.734
DFC	0.7951	0.7586	0.8281	0.8	0.791	0.7788	0.903
DWFC	0.8525	0.8276	0.875	0.8571	0.8485	0.8421	0.9316

Table 3: The achieved classification results using different methods on UCLA dataset.

Method	AAC	SEN	SPE	PPV	NPV	F	AUC
PC	0.7143	0.8	0.6047	0.7213	0.7027	0.7586	0.8085
DFC	0.7857	0.7455	0.8372	0.8542	0.72	0.7961	0.8457
DWFC	0.8061	0.8	0.814	0.8462	0.7609	0.8224	0.8609

In addition, we also compare the proposed methods with some other state-of-the-art methods, which also used fMRI images collected from the New York University Langone Medical Center, for ASD classification. For example, Wee et al. [37] used Temporally Distinct Functional Connectivity Networks (TDFCN) and support vector machine with three different kernels (i.e., linear, Radial Basis Function (RBF), and polynomial) to identify ASD patients; Wang et al.[4] combined the white matter and grey matter tissue volumes of each brain region as the classification features, then a novel CCA-based Graph Matching Sparse Group Lasso (GMSGL) feature selection method was adopted to classify ASD; Zhao et al.[3] integrated MRI and fMRI features, and used HSL-CCA method to select the most discriminative features, finally the linear SVM with default parameter was used for classification. The classification results of these methods were listed in **Table 4.** As we can see from **Table 4**, compared against other classification.

Table 4: The classification results about different methods on ASD classification on NYU dataset.

Method	ACC	SEN	SPE	PPV	NPV
TDFCN(Linear)	0.707	0.814	0.612	0.79	0.648
TDFCN(RBF)	0.717	0.605	0.816	0.743	0.702
TDFCN(polynomial)	0.641	0.814	0.49	0.583	0.75
GMSGL	0.754	0.7463	0.7596	0.7478	0.762
HSL-CCA	0.816	0.811	0.825	0.815	0.823
DWFC	0.8525	0.8276	0.875	0.8571	0.8485

Frameworks, our proposed method achieved the best classification performance, in terms of classification accuracy, sensitivity, specificity or PPV, NPV. Specifically, the classification accuracy obtained by the proposed method nearly 14% higher than that by TDFCN, which again demonstrating the efficacy of proposed method.

Comparison between SVM and other classifiers

SVM is a popular classification algorithm in machine learning and pattern recognition field, and it has widely used in disease diagnosis. Besides, random forest (RF) and K nearest neighbors (KNN) were also draw researchers' attention. To investigate the classification performance of different classifiers, additional experiments were performed on other two classification algorithms. The results were presented in **Figure 4**. As observed in the figure, SVM achieved the highest classification accuracy on both two datasets. Specially, there is a great gap between sensitivity and specificity when using RF or KNN as classifier, primary reason of the phenomenon is due to the imbalance of data, but it didn't appear when SVM as the classifier. These may be the reason why various studies used SVM as the classifier to identify diseases.

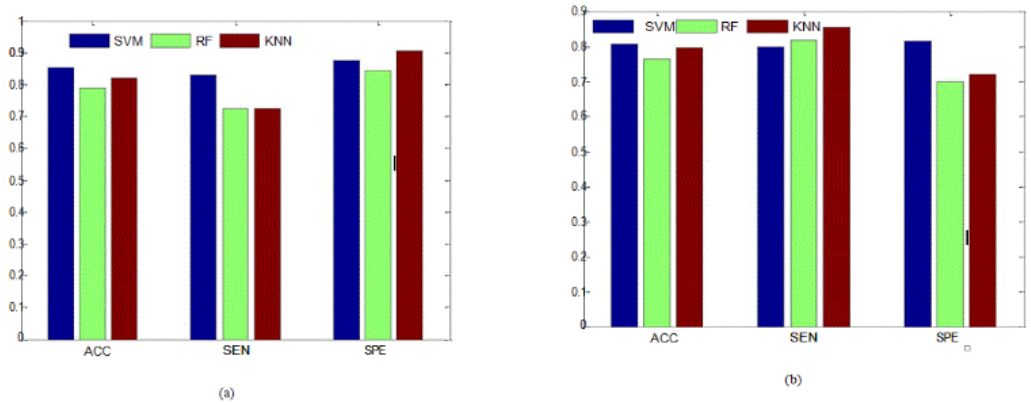

Figure 4: The classification results of three different classifiers. (a)NYU; (b)UCLA.

Effect of window length N

Since window length may affect final classification performance, the window length typically vary from 12.5 to 240 s in previous studies [38,39]. Therefore, to find out the most optimal value of N for the final classification accuracy, we set N range from 15 to 100 with an increment of 5. The classification accuracy was summarized in **Figure 5**. It's not difficult found that when N is 30 and 35 for NYU and UCLA dataset, the highest classification accuracy was achieved.

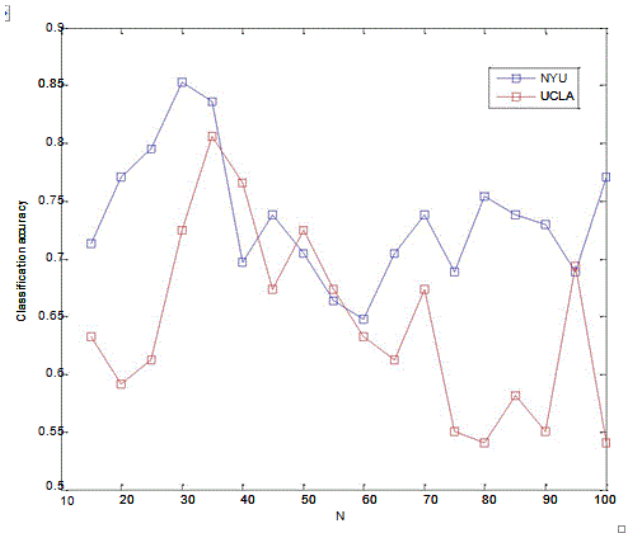

Figure 5: The obtained classification accuracy when N has different values.

Most important regions

The weight of selected brain regions for final classification was showed in **Figure 6**. Although the experiments were conducted on two different datasets, many important brain regions were included both of the two experiments, such as amygdala, angular gyrus, and precuneus, besides, some brain regions from cerebellum were also included, such as Lobule IX of cerebellar hemisphere, Lobule X of vermis, all of these were play a key role in ASD identification.

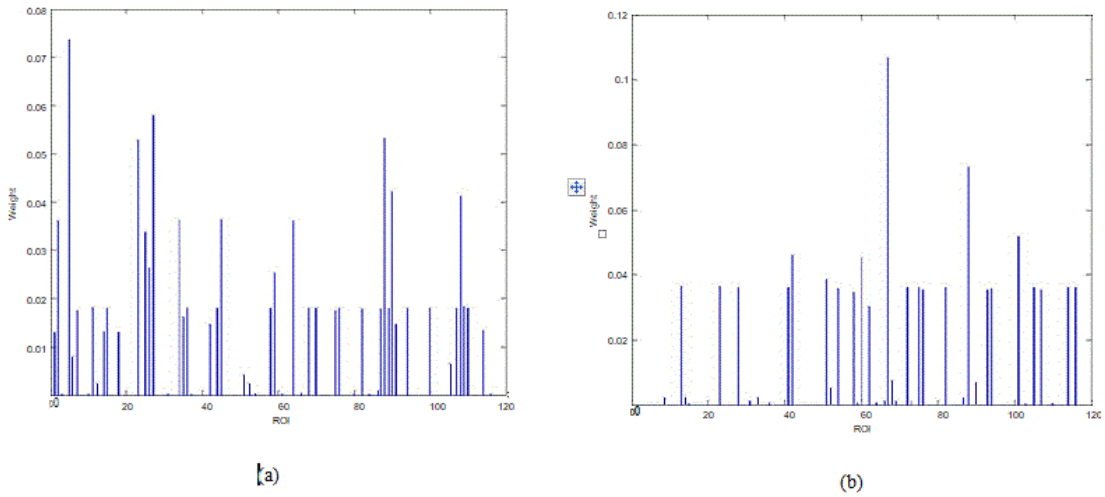

Figure 6: The weight of selected brain regions for final classification. (a)NYU; (b)UCLA.

The amygdala plays a key role in social behavior and emotion. It's mainly function appears to be the linking of perceptual representations to cognition and behavior on the basis of the emotional or social value of the stimuli [40]. Social impairment is one of the important dysfunctions of autism, previous studies [41,42] have reported amygdala volumes abnormality in autism. The precuneus is an intriguing cortical area, plays an important role in visuospatial imagery, episodic memory retrieval and self-processing operations [43]. Besides, cerebellar volume abnormality was found in individual with autism [41,42,44]. For example, Sparks et al. [42] conducted an experiment on 71 children (of which 45 ASD patients) between 3 and 4 years of age, found increased cerebellar volume in ASD group, and the same finding was reported in Piven's study on adult individuals.

Discussion

Connectivity network analysis method has widely used in diseases identification. The key point is how to establish the network. Currently, the Pearson's correlation based network is the most common approach to investigate the interaction relationship between different brain regions. With the development of research, more and more evidence shows that the correlation between regions is time-varying. To some extent, the changes in FC have been linked to changes in cognitive or vigilance states [45-47]. To capture the changes, DFC method was proposed. Previous studies reported on disease-related alterations in DFC suggested that the temporal features of FC could serves as a disease biomarker [48], so since DFC network was proposed, it has widely used in diagnosis of mild cognitive impairment (MCI) [49], epilepsy [39]. To our knowledge, DFC method has not utilized in detection of ASD in previous studies. And conventional DFC has the drawback that all observations within the time window weighted equally. To address the problem, in this work, we proposed a DWFC method to distinguish patients with ASD from normal controls. Different from the conventional FC method based on PC that considers pairwise relationship on entire scan session, DWFC can capture the dynamic changes over the scan session; meanwhile, the different contribution of different time point was also taken into account. Results indicated that our proposed framework could deliver significant higher classification accuracy than conventional FC and DFC in distinguishing ASD patients from normal controls.

It is noteworthy that high sensitivity is very important for the purpose of measure the power of the proposed classification framework, because there would generate different costs for misclassifying a normal control to be a patient or misclassifying a patient to a healthy person. Compared with the former, the latter may cause some more severe consequences, because if a patient is misdiagnosed as a healthy person, necessary treatments to delay or cure the disease may not be provided on time during the critical treatment period. This would accelerate the progression of disease from mild to severe, a point where no effective treatment is available, eventually causing death of patient [50].

Many psychiatric disorders are thought to be brain connectivity disorders. **Figure 7** shows the most discriminative inter-regional functional features selected from rs-fMRI. The thickness of each arc in the figure represents the discriminating power of the corresponding connection, and the color of each arc in the figure is randomly assigned just for better visualization. It can be observed from the figure that many of the connection located in frontal area and temporal regions. Previous studies have found abnormal level of connection in regional activation in the frontal regions in autism [51-53]. Keller et al. [54] have reported reductions in the structural integrity of white matter in individual with autism, in frontal lobe areas near the corpus callosum. Temporal regions are implicated in social perception and language abilities that are impaired in autism [55]. Previous studies [56,57] have reported bilateral temporal hypo perfusion in autistic children.

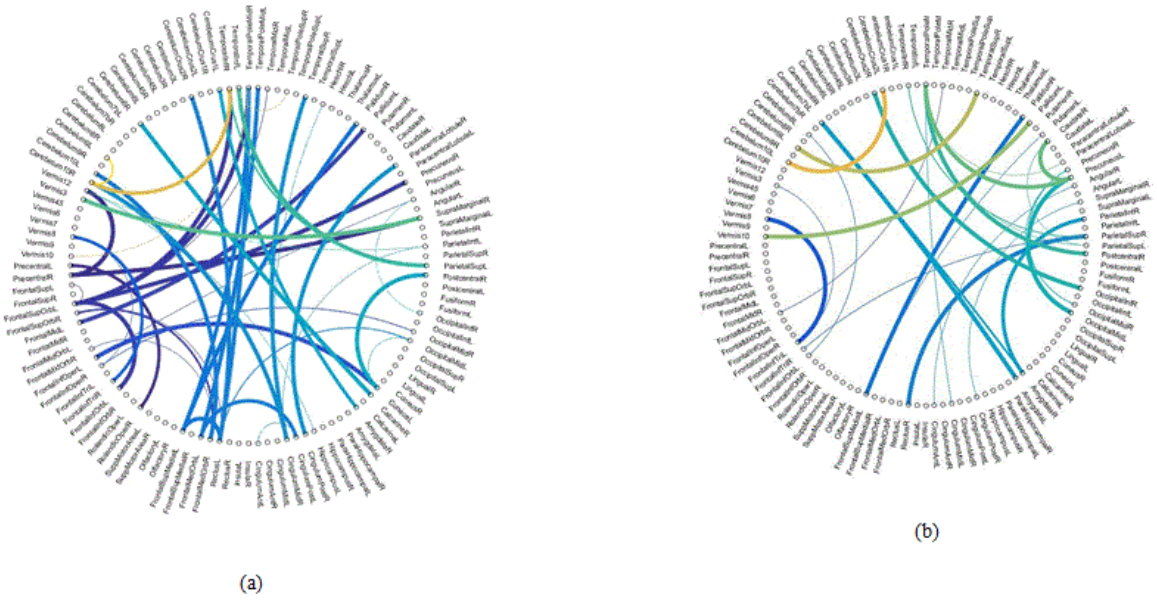

Figure 7: The most discriminative features used in classification. (a) NYU; (b) ULCA.

There is a strange phenomenon is that boys were almost 5 times more likely to be identified with ASD than girls. To investigate the phenomenon whether related to connectivity, average connectivity matric based on PC was calculated in **Figure 8**. It can be observed that there exists stronger connection between frontal and temporal area, frontal and cerebellum regions, temporal and cerebellum regions in female than male, which may provide a reasonable explanation to the phenomenon.

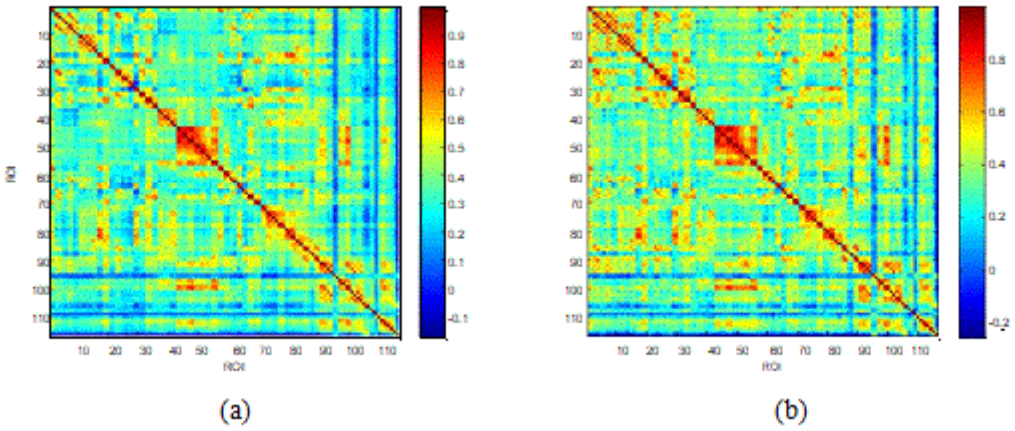

Figure 8: Average FC matric on ASD subjects. (a)Male; (b) Female.

Although a promising result was achieved by the proposed framework, it has some limitations. First, sample size is relatively small for the pattern classification tasks, validation on larger datasets is demanding. Second, the proposed method is based on fMRI images, some other imaging modalities, such as Diffusion Tensor Imaging (DTI), structural Magnetic Resonance Imaging (sMRI), and Positron Emission Tomography (PET), and some other information, such as eye movement, facial expressions should be taken into account to obtain a more comprehensive measure of the risk of ASD to aid the early detection for ASD. For example, Liu et al. [58] identifying children with ASD based on subjects' face using a machine learning framework, and a promising result was achieved. If we can combine brain data with face images, an unexpected result might be obtained. Third, most of the samples used in current work are age between 7 to 15, previous study [59] reported that behavioral abnormalities can be observed before the age of 30 months in ASD patients, if more samples under the age of 30 months can included in the dataset, a more reasonable framework may obtained.

Conclusion

In this paper, a dynamic weighted FC method was proposed to effectively identify patients with ASD from healthy normal controls. Compared with the conventional FC study, the method can better capture the dynamic characteristic and time point specificity. The experimental results confirmed the effectiveness of the proposed method; it also demonstrated the superiority of the proposed method over other state-of-the-art methods. Furthermore, the proposed method can be extended to diagnose other mental disorders, such as Parkinson disease, Alzheimer's disease, Attention Deficit Hyperactivity Disorder (ADHD), schizophrenia, and so on.

Acknowledgments

This work was supported by the National Science Fund of China under Grant Nos. U1713208, and Program for Changjiang Scholars.

References

1. Geschwind DH, Levitt P (2007) Autism spectrum disorders: Developmental disconnection syndromes. Curr Opin Neurobiol 17: 103-111.
2. Ecker C, Marquand A, Mourão-Miranda J, Johnston P, Daly EM, et al. (2010) Describing the brain in autism in five dimensions-magnetic resonance imaging-assisted diagnosis of autism spectrum disorder using a multiparameter classification approach. J Neurosci 30: 10612-10623.
3. Zhao F, Qiao L, Shi F, Yap PT, Shen D (2016) Feature fusion via hierarchical supervised local CCA for diagnosis of autism spectrum disorder. Brain Imaging Behav: 1-11.
4. Wang L, Wee CY, Tang X, Yap PT, Shen D (2016) Multi-task feature selection via supervised canonical graph matching for diagnosis of autism spectrum disorder. Brain Imaging Behav 10: 33-40.
5. Guilmatre A, Dubourg C, Mosca A-L, Legallic S, Goldenberg A, et al. (2009) Recurrent rearrangements in synaptic and neurodevelopmental genes and shared biologic pathways in Schizophrenia, Autism, And Mental Retardation. Arch Gen Psychiatry 66: 947-956.
6. Wee CY, Wang L, Shi F, Yap PT, Shen D (2014) Diagnosis of autism spectrum disorders using regional and interregional morphological features. Hum Brain Mapp 35: 3414-3430.
7. Menon V (2011) Large-scale brain networks and psychopathology: A unifying triple network model. Trends Cogn Sci 15: 483-506.
8. Mostapha M, Casanova M, Gimel'farb G, El Baz A (2015) Towards Non-invasive Image-Based Early Diagnosis of Autism. Springer. pp: 160-168.
9. Jie B, Wee CY, Shen D, Zhang D (2016) Hyper-connectivity of functional networks for brain disease diagnosis. Med Image Anal 32: 84-100.
10. Gallego JE, Solé CJ, Vialatte FB, Elgendi M, Cichocki A, et al. (2015) A hybrid feature selection approach for the early diagnosis of Alzheimer's disease. J Neural Eng 12: 016018.
11. Adeli E, Shi F, An L, Wee C-Y, Wu G, et al. (2016) Joint feature-sample selection and robust diagnosis of Parkinson's disease from MRI data. NeuroImage 141: 206-219.
12. Rashid B, Arbabshirani MR, Damaraju E, Cetin MS, Miller R, et al. (2016) Classification of schizophrenia and bipolar patients using static and dynamic resting-state fMRI brain connectivity. NeuroImage 134: 645-657.
13. Shim M, Hwang HJ, Kim DW, Lee SH, Im CH (2016) Machine-learning-based diagnosis of schizophrenia using combined sensor-level and source-level EEG features. Schizophr Res 176: 314-319.
14. Iidaka T (2015) Resting state functional Magnetic Resonance Imaging and neural network classified Autism and control. Cortex 63: 55-67.
15. Chen H, Duan X, Liu F, Lu F, Ma X (2016) Multivariate classification of autism spectrum disorder using frequency-specific resting-state functional connectivity: A multi-center study. Prog Neuropsychopharmacol Biol Psychiatry 64: 1-9.
16. Subbaraju V, Suresh MB, Sundaram S, Narasimhan S (2017) Identifying differences in brain activities and an accurate detection of autism spectrum disorder using resting state functional-magnetic resonance imaging: A spatial filtering approach. Med Image Anal 375-389.
17. Hutchison RM, Womelsdorf T, Allen EA, Bandettini PA, Calhoun VD, et al. (2013) Dynamic functional connectivity: Promise, issues, and interpretations. Neuroimage 80: 360-378.
18. Lindquist MA, Xu Y, Nebel MB, Caffo BS (2014) Evaluating dynamic bivariate correlations in resting-state fMRI: A comparison study and a new approach. Neuroimage 101: 531-546.
19. Kudela M, Harezlak J, Lindquist MA (2017) Assessing uncertainty in dynamic functional connectivity. NeuroImage 149: 165-177.
20. Di Martino A, Yan CG, Li Q, Denio E, Castellanos FX, et al. (2014) The autism brain imaging data exchange: Towards a large-scale evaluation of the intrinsic brain architecture in autism. Mol Psychiatry 19: 659-667.
21. Chao-Gan Y, Yu-Feng Z (2010) DPARSF: A MATLAB toolbox for "pipeline" data analysis of resting-state fMRI. Front Syst Neurosci 14;4:13.
22. Song XW, Dong ZY, Long XY, Li SF, Zuo XN, et al. (2011) REST: A toolkit for resting-state functional Magnetic Resonance Imaging data processing. PloS One 6: e25031.
23. Zeng LL, Shen H, Liu L, Hu D (2014) Unsupervised classification of major depression using functional connectivity MRI. Hum Brain Mapp 35: 1630-1641.
24. Tzourio MN, Landeau B, Papathanassiou D, Crivello F, Etard O, et al. (2002) Automated anatomical labeling of activations in SPM using a macroscopic anatomical parcellation of the MNI MRI single-subject brain. Neuroimage 15: 273-289.
25. Zeng LL, Shen H, Liu L, Wang L, Li B, et al. (2012) Identifying major depression using whole-brain functional connectivity: A multivariate pattern analysis. Brain 135: 1498-1507.
26. Kucyi A, Salomons TV, Davis KD (2013) Mind wandering away from pain dynamically engages antinociceptive and default mode brain networks. Proc Natl Acad Sci 110: 18692-18697.
27. Sadaghiani S, Poline JB, Kleinschmidt A, D'Esposito M (2015) Ongoing dynamics in large-scale functional connectivity predict perception. Proc Natl Acad Sci 8463-8468.
28. Pozzi F, Di Matteo T, Aste T (2012) Exponential smoothing weighted correlations. The European Physical Journal B 85: 1-21.
29. Tibshirani R (1996) Regression shrinkage and selection via the lasso. Journal of the Royal Statistical Society: Series B (Methodological) banner 267-288.

30. Chang, ChihChung, Lin, ChihJen (2011) LIBSVM: A library for support vector machines. Acm Transactions on Intelligent Systems & Technology 2: 389-396.

31. Cortes C, Vapnik V (1995) Support-vector networks. Machine learning 20: 273-297.

32. Vapnik VN, Vapnik V (1998) Statistical learning theory: Wiley New York.

33. Liu Z, Xiao X, Yu DJ, Jia J, Qiu WR, et al. (2016) pRNAm-PC: Predicting N 6-methyladenosine sites in RNA sequences via physical–chemical properties. Anal Biochem 497: 60-67.

34. Chen W, Ding H, Feng P, Lin H, Chou KC (2016) iACP: A sequence-based tool for identifying anticancer peptides. Oncotarget 7: 16895-16909.

35. Wee CY, Yap PT, Zhang D, Wang L, Shen D (2014) Group-constrained sparse fMRI connectivity modeling for mild cognitive impairment identification. Brain Struct Funct 219: 641-656.

36. Haller S, Badoud S, Nguyen D, Barnaure I, Montandon M, et al. (2013) Differentiation between Parkinson disease and other forms of Parkinsonism using support vector machine analysis of susceptibility-weighted imaging (SWI): Initial results. Eur Radiol 23: 12-19.

37. Wee CY, Yap PT, Shen D (2016) Diagnosis of autism spectrum disorders using temporally distinct resting- State functional connectivity networks. CNS Neurosci Ther 22: 212-219.

38. Shakil S, Lee C-H, Keilholz SD (2016) Evaluation of sliding window correlation performance for characterizing dynamic functional connectivity and brain states. NeuroImage 133: 111-128.

39. Liu F, Wang Y, Li M, Wang W, Li R, et al. (2016) Dynamic functional network connectivity in idiopathic generalized epilepsy with generalized tonic: clonic seizure. Hum Brain Mapp 38(2):957-973.

40. Adolphs R (2001) The neurobiology of social cognition. Current Opinion in Neurobiology 11: 231-239.

41. Herbert M, Ziegler D, Deutsch C, O'brien L, Lange N, et al. (2003) Dissociations of cerebral cortex, subcortical and cerebral white matter volumes in autistic boys. Brain 126: 1182-1192.

42. Sparks B, Friedman S, Shaw D, Aylward E, Echelard D, et al. (2002) Brain structural abnormalities in young children with autism spectrum disorder. Neurology 59: 184-192.

43. Cavanna AE, Trimble MR (2006) The precuneus: A review of its functional anatomy and behavioural correlates. Brain 129: 564-583.

44. Piven J, Saliba K, Bailey J, Arndt S (1997) An MRI study of autism: The cerebellum revisited. Neurology 49: 546-551.

45. Betti V, Della Penna S, De Pasquale F, Mantini D, Marzetti L, et al. (2013) Natural scenes viewing alters the dynamics of functional connectivity in the human brain. Neuron 79: 782-797.

46. Thompson GJ, Magnuson ME, Merritt MD, Schwarb H, Pan WJ, et al. (2013) Short-time windows of correlation between large-scale functional brain networks predict vigilance intraindividually and interindividually. Hum Brain Mapp 34: 3280-3298.

47. Wilson RS, Mayhew SD, Rollings DT, Goldstone A, Przezdzik I, et al. (2015) Influence of epoch length on measurement of dynamic functional connectivity in wakefulness and behavioural validation in sleep. NeuroImage 112: 169-179.

48. Jones DT, Vemuri P, Murphy MC, Gunter JL, Senjem ML, et al. (2012) Non-stationarity in the "resting brain's" modular architecture. PloS One 7: e39731.

49. Wee CY, Yang S, Yap PT, Shen D. (2016) Initiative AsDN Sparse temporally dynamic resting-state functional connectivity networks for early MCI identification. Brain Imaging Behav 10: 342-356.

50. Wee CY, Yap PT, Zhang D, Denny K, Browndyke JN, et al. (2012) Identification of MCI individuals using structural and functional connectivity networks. Neuroimage 59: 2045-2056.

51. Horwitz B, Rumsey JM, Grady CL, Rapoport SI (1988) The cerebral metabolic landscape in autism: Intercorrelations of regional glucose utilization. Arch Neurol 45: 749-755.

52. Luna B, Minshew N, Garver K, Lazar N, Thulborn KR, et al. (2002) Neocortical system abnormalities in autism: An fMRI study of spatial working memory. Neurology 59: 834-840.

53. Koshino H, Carpenter PA, Minshew NJ, Cherkassky VL, Keller TA, et al. (2005) Functional connectivity in an fMRI working memory task in high-functioning autism. Neuroimage 24: 810-821.

54. Keller TA, Kana RK, Just MA (2007) A developmental study of the structural integrity of white matter in autism. Neuroreport 18: 23-27.

55. Gendry MI, Zilbovicius M, Boddaert N, Robel L, Philippe A, et al. (2005) Autism severity and temporal lobe functional abnormalities. Ann Neurol 58: 466-469.

56. Ohnishi T, Matsuda H, Hashimoto T, Kunihiro T, Nishikawa M, et al. (2000) Abnormal regional cerebral blood flow in childhood autism. Brain 123: 1838-1844.

57. Zilbovicius M, Boddaert N, Belin P, Poline JB, Remy P, et al. (2000) Temporal lobe dysfunction in childhood autism: A PET study. Am J Psychiatry 157: 1988-1993.

58. Liu W, Li M, Yi L (2016) Identifying children with autism spectrum disorder based on their face processing abnormality: A machine learning framework. Autism Res 9: 888-898.

59. Palmen SJ, Van EH (2004) Review on structural neuroimaging findings in autism. Journal of Neural Transmission 111: 903-929.